Influence of Annealing Temperature on Y_2O_3:SiO_2 Nanocomposite Prepared by Sol–Gel Process

R. Ahlawat* and P. Aghamkar
Department of Physics, Materials Science Lab., Ch. Devi Lal University, Sirsa-125055, Haryana, India

(Received February 22, 2013; in final form May 15, 2014)

Oxide nanoparticles embedded in a polymer matrix produce nanocomposites which are useful for optics and electronic applications. Yttrium oxide nanoparticles have received much attention due to their various properties and are significantly used in fundamental and application oriented fields. The present paper reports the influence of annealing temperature on the Y_2O_3:SiO_2 nanocomposite prepared by sol–gel process. $Y(NO_3)_3{\cdot}4H_2O$ and tetraethoxysilane were used as precursors and obtained powdered form of Y_2O_3:SiO_2 composite. The powder sample was annealed at 500 °C and 900 °C for 6 h which were characterized by X-ray diffraction, Fourier transform infrared and transmission electron microscope. X-ray diffraction data described that the broadening of peaks decreases with increase in annealing temperature which may be due to the increase in particle size. Sample analyzed by Fourier transform infrared and transmission electron microscopy confirmed the grain size dependence on annealing temperature. Cubic phase of yttrium oxide crystal structure was obtained within the silica matrix. The nanocrystallites size has been calculated using Debye–Scherrer formula, Williamson–Hall plot and transmission electron micrographs and compared at two different temperatures (a) 500 °C and (b) 900 °C.

DOI: 10.12693/APhysPolA.126.736
PACS: 61.46.Bc, 61.46.Df, 78.67.Bf

1. Introduction

Oxide nanoparticles have attractive optical, electric, and chemical applications compared to the bulk of the same material. These materials have numerous applications for developing new devices [1–4]. In nanomaterials, particle size reduces, the surface to volume ratio dominates and that determines most of the properties of nanomaterials. Yttrium oxide is one of the seventeen rare earth oxides which is a super refractory oxide that finds use in a variety of applications including optics, display devices, X-ray imaging, core-shell materials and also as additive for liquid phase sintering of ceramics [5, 6]. Nanocrystalline Y_2O_3 has been widely investigated, due to its interesting applications in the field of phosphors for lighting and for cathode ray tube [7, 8]. The surface of nanoparticles can be changed either by chemical reactions or by dispersing the particles in a polymer or glass matrix. From this point of view, silica represents the ideal candidate for rare earth metals both because of its transparency and its stabilizing effect on the nanoparticles, protecting them aggregation. Some authors have represented the use of silica for coating [9] or as a dispersing medium [10] by impregnation, for doped yttrium nanoparticles. Nanocrystalline Y_2O_3 has already been synthesized by various methods such as hydrothermal [11], combustion synthesis [12], and co-precipitation [13] techniques.

In the present article, sol–gel technique is being used for the preparation of Y_2O_3 nanocrystallites in a silica matrix. The sol–gel process combines the advantage of lower temperature and possibility of making of finely dispersed powders, films, fibers and coating [14]. Rare-earth oxides, due to their special properties, have also been used in many fields such as ceramic industry and sensors. As we know, the smaller the particles size, the larger the specific surface area, and the higher the activity. Thus synthesis of different structure/phases of rare oxides nanocrystallites is in great demand to fulfill the requirements of technology and industry. Some researchers [15] synthesized Y_2O_3:SiO_2 samples by sol–gel method but they observed that yttrium nanoparticles do not grow with thermal treatment even at 900 °C and 1300 °C. The development of new rare-earth oxides and silica binary systems are important not only for technological reasons but also for obtaining a better understanding. Literature survey [16, 17] reveals that formation of rare-earth oxides/silicates inside or at the surface of SiO_2 matrix depends on the synthesis method, rare-earth oxide and silica molar ratio and thermal/pressure treatment. In the present work, we investigated the structural properties of Y_2O_3:SiO_2 samples obtained by sol–gel methods and examined the influence of heat treatment on nanoparticles through X-ray diffraction (XRD) and Fourier transform infrared (FTIR) techniques which is further confirmed by transmission electron microscopy (TEM).

2. Experimental

2.1. Sample preparation

Y_2O_3:SiO_2 nanocomposite has been prepared by using the sol–gel technique. The high purity reagents: tetraethoxysilane (Aldrich 99.999), ethanol (Merck 99.9%) and double distilled water were mixed in the presence of hydrochloric acid as catalyst. To prepare the sample the molar ratio of starting solution was taken as 2.30: 0.72: 0.30: 0.027 for H_2O:C_2H_5OH: HCl: TEOS and 0.56 M yttrium nitrate tetra hydrate with concentration

*corresponding author; e-mail: rachnaahlawat2003@yahoo.com

of HNO_3 was introduced in the pre-hydrolyzed solution under heating. The solution was kept at room temperature for three weeks where aging occurred. The aging process allows further shrinkage and stiffening of the gel. The samples were further dried at 100 °C for 24 h and the powder form of the samples was obtained by pestle and mortar. The powder form of the sample was annealed in high temperature programmable furnace NSW 103 at different temperature i.e. from room temperature up to 500 °C and 900 °C for 6 h in air and then cooled up to room temperature by its own.

2.2. Characterization

The prepared samples were characterized by an X'pert Pro X-ray Diffractometer with Cu K_{α_1} radiation in the range of 5°–80° in steps of 0.017° (40 mA, 45 kV) for the determination of crystalline structure of nanocomposites. Infrared spectra of annealed samples at 500 °C and 900 °C were collected from Perkin Elmer Spectrum 400 spectrophotometer in 4000–400 cm^{-1} range. FTIR spectrometer was used for functional group analysis. The morphological investigations of the annealed samples were performed by Hitachi-4500 transmission electron microscope at an accelerating voltage of 80 V.

3. Result and discussion

3.1. XRD analysis

The XRD patterns shown in Fig. 1 illustrate the effect of annealing temperature on the structural evolution of Y_2O_3:SiO_2 composites prepared by sol–gel process. XRD results indicate that crystallinity of the prepared sample increases with temperature without any reaction between the SiO_2 and Y_2O_3. The sample (a) annealed at 500 °C for 6 h presents diffraction peak at $2\theta \approx 29.25°$ (222) along with weak peaks $2\theta \approx 33.85°$ (400), 48.58° (440), 57.77° (622) and $2\theta \approx 20.62°$ (211) which indicates that cubic Y_2O_3 crystal structure (in accordance to JCPDS card no. 41-1105) grows well. Check cell program was used to find the Miller indices of respective peaks, which confirmed the structure of cubic Y_2O_3 (α-Y_2O_3) having lattice constant $a = 10.56$ Å with C-M_2O_3 type structure and space group $Ia3$ (T_h^7) [18]. The single peak of crystalline silica has been observed at 25.64°. The sample (b) annealed at 900 °C illustrated the same pattern as that of (a) in which no other phase has been observed which reveals that no reaction occurred between yttrium oxide and silica even annealing after 900 °C. Here, it is worth pointing out that the literature showed that if the samples were annealed at 1000 °C or higher temperature a reaction between Y_2O_3 and SiO_2 occurred, resulting in the formation of impurities like Y_2SiO_5 [19]. Therefore, we have limited the annealing temperature at 900 °C in this work.

We expect that during annealing at 900 °C, individual nanostructures merge together and the activation energy becomes much larger. Therefore cross-grain boundaries diffusion dominates over surface and volume diffusion process and eventually crystallinity increases. The prepared samples were agglomeration of many primary particles and it results in increase in crystalline size as

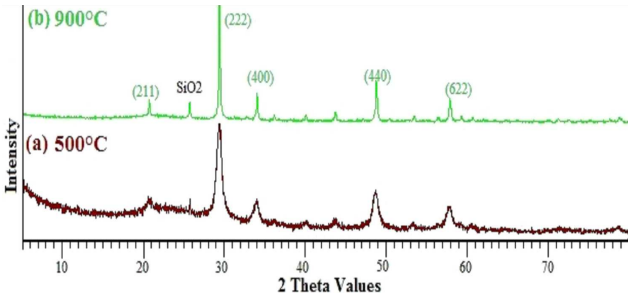

Fig. 1. XRD patterns of the Y_2O_3:SiO_2 sample annealed at 500 °C (a) and 900 °C (b).

well as the intensity of characteristic peaks increases. It is also observed that broadening of peaks decreases with the increase in temperature. The sharp and strongest diffraction peak around $2\theta \approx 29.25°$ was employed to estimate the mean crystallite size of the prepared samples from the well known Debye–Scherrer (D–S) equation [20]:

$$D_{hkl} = K\lambda/(\beta \cos\theta), \tag{1}$$

where λ is the X-ray wavelength, θ is the diffraction angle, K is the shape factor which is 0.9 for uniform small size crystal, and D_{hkl} means the size along (hkl) plane. Here we have calculated average crystallite sizes of Y_2O_3:SiO_2 sample which is ≈ 10 nm for the sample annealed at 500 °C and ≈ 30 nm for that annealed at 900 °C and details are given in Table.

TABLE

Calculation of particle size at different temperatures.

Temperature	D–S formula	W–H plot	TEM/histograms	Strain (ε)
500 °C	10 ± 2 nm	13 nm	0.4 ± 2 nm	1.41×10^{-3}
900 °C	30 ± 2 nm	33 nm	27 ± 2 nm	1.05×10^{-3}

The XRD profile shown in Fig. 1 shows some broadening which may be due to lattice strain [21]. When the sample was annealed at higher temperature, the lattice strain is reduced. Due to the small crystallite size and strain present in the materials, the XRD peak broadening can be distinguished from the Williamson–Hall (W–H) plot. Here, the crystallite size has also been estimated using W–H equation given as

$$\beta_{hkl} \cos\theta_{hkl} = K\lambda/d + 4\varepsilon \sin\theta_{hkl}, \tag{2}$$

where K, λ, and θ_{hkl} are having their usual meaning as mentioned in Eq. (1), d is the average crystallite size. The graph has been plotted between $4\sin\theta_{hkl}$ and β_{hkl} $\cos\theta_{hkl}$ as shown in Fig. 2. The value of the strain was estimated from slope of the line and the crystallite size from the intersection with the vertical axis. The estimated crystallite size of the composites from this method was in agreement with the Debye–Scherrer equation and TEM morphological results. From the W–H plot, it was observed that the strain values are very small and hence the strain has negligible effect in XRD broadening.

The above result suggests that the thermal treatment Y_2O_3:SiO_2 composites system, synthesized by sol–gel

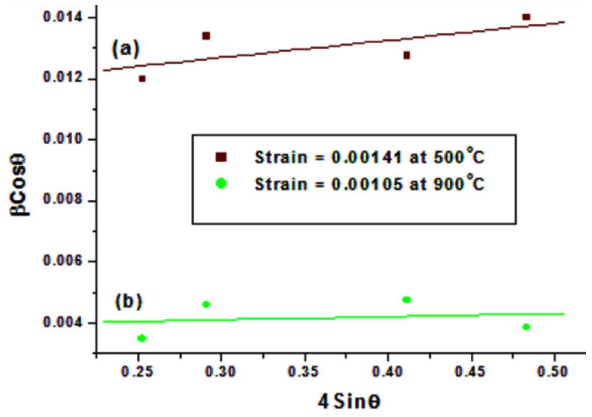

Fig. 2. W–H plot for the Y_2O_3:SiO_2 sample annealed at 500 °C (a) and 900 °C (b).

technique, at temperature of 900 °C produces Y_2O_3:SiO_2 nanocomposite system with increased crystallite size and distinct grain boundaries.

3.2. FTIR analysis

Figure 3 shows FTIR spectra of Y_2O_3:SiO_2 composite sample annealed at 500 °C (a) and 900° (b). The infrared absorption spectra of the heat treated samples provide some important information about the structural changes. Figure 3 shows broad absorption bands nearly at 1098, 804, and 445 cm^{-1}. These bands are attributed to the asymmetric, symmetric stretching vibration, and bending vibrations of the Si–O–Si bond [17] in both the samples. While characteristic absorption peaks of Y–O (metal-oxygen) appeared at 405 and 506 cm^{-1} in the FTIR spectra [22]. The absorption band of O–H stretching vibrations appears around 3550 and 1625 cm^{-1} of absorbed water. As the temperature was increased, the intensity of the absorption band becomes less, may be due to vaporization, and a characteristic peak of Y–O becomes strong and sharp in well agreement with XRD results.

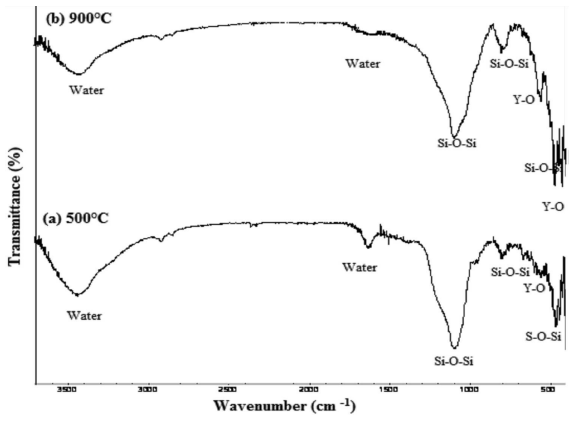

Fig. 3. FTIR spectra of Y_2O_3:SiO_2 sample annealed at 500 °C (a) and 900 °C (b).

The three parts of spectra undergo the expected modifications due to the thermal treatment, i.e. exhibiting a decrease in the shoulder at 960 cm^{-1}, due to the stretching of silanol groups, and a less evident increase in the band at 795 cm^{-1}, ascribed to the bending of Si–O–Si [15]. In particular, the band at 960 cm^{-1} disappears in the spectrum of sample (b). This behavior is typical of the silica condensation process with heat treatment. Moreover, the water signals are visible in the IR spectra of the nanocomposite even after a treatment up to 900 °C. It is likely that the presence of water is partially due to the hydrophilicity of the samples or impure KBr used in sampling for FTIR. However, these signals attenuate but do not disappear after heating the samples at 1000 °C (drying temperature) during the spectra collection, suggesting that some water molecules remain inside the pores of the material.

3.3. TEM analysis

Figure 4 shows the TEM micrographs of the Y_2O_3:SiO_2 sample annealed at 500 °C (a) and 900 °C (b). Highly agglomerated nanocrystallites are clearly visible in both the micrographs. Several nanocrystallites are agglomerated to form a single particle and therefore the particle size distribution of samples lies in the broad range as shown in the histograms 4c and d. The TEM images confirm the large particle size distribution and grain growth process in the annealed samples. The sample (a) annealed at 500 °C for 6 h produces 3–7 nm nanocrystallites with narrow size distribution, as shown in Fig. 4a. Sample (b) annealed at 900 °C for 6 h gradually grew into large and almost spherical particles, about 27 nm (average) in diameter, as shown in Fig. 4b.

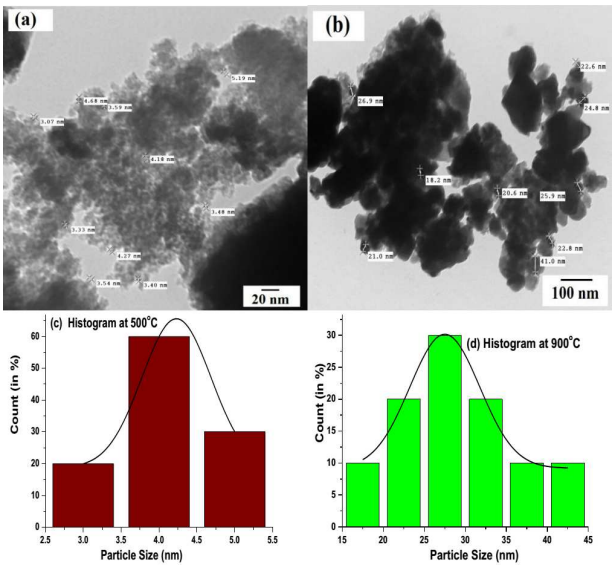

Fig. 4. TEM micrograph for the Y_2O_3:SiO_2 sample annealed at (a) 500 °C and (b) 900 °C. (c) Particle size distribution at 500 °C, (d) 900 °C.

One may notice that some nanocrystallites are very small ≈ 18 nm and few are having size ≈ 41 nm range.

In sample (b), the grain growth indicated the diffusivity of grain boundary of obtained nanocrystallites. The average nanocrystallites sizes indicated in the micrographs 4a and b have been measured by inbuilt software in Hitachi--4500 Transmission Electron Microscope. It is evident from Fig. 4 that thermal treatment of the sample at comparatively high temperature (900 °C) provides much improved dispersion of Y_2O_3 in the silica matrix. The above result infer that the crystallite structure of Y_2O_3:SiO_2 composite obtained by sol–gel method can be controlled by selecting correctly both the thermal treatment and used precursors.

4. Conclusion

Using sol–gel method Y_2O_3:SiO_2 nanocomposite was successfully obtained upon thermal treatment in air at two different temperatures. XRD data analyzed that the cubic phase of Y_2O_3 crystal structure was well grown within the silica matrix. The nanocrystallites size have been calculated using D–S formula, W–H plot and TEM micrographs and compared at two different temperatures (a) 500 °C and (b) 900 °C. The histograms for particle size distribution have been plotted in the range 2.5–5.5 nm and 15–45 nm, respectively. The Gaussian fit was employed in these histograms to obtain the average nanocrystallite size. In XRD with rise in temperature the peak broadening increases which emphasizes the increased particle size due to agglomeration of nanoparticles which was further confirmed by transmission electron microscope. Functional groups have been investigated by FTIR spectra and it shows that the absorption bands broadened as the particle size decreases. The characteristic absorption peaks of Si–O–Si symmetric, asymmetric and bending vibrations are nearly at the position in both the annealed samples. Yttrium-oxygen characteristic absorption band appeared at 405 and 506 cm^{-1}.

References

[1] K. Ariga, J.P. Hill, M.V. Lee, A. Vinu, R. Charvet, S. Acharaya, *Sci. Technol. Adv. Mater.* **9**, 014109 (2008).

[2] G.S. Yi, G.M. Chow, *J. Mater. Chem.* **15**, 4460 (2005).

[3] J.H. Zeng, J. Su, Z.H. Li, R.X. Yan, Y.D. Li, *Adv. Mater.* **17**, 2119 (2005).

[4] J.W. Stouwdam, F.C.J.M.V. Veggel, *Nano Lett.* **2**, 733 (2002).

[5] Y. Wang, Q. Zeng, S. Hu, K. Wu, J. Jiang, *J. Rare Earths* **28**, 176 (2010).

[6] R. Dai, Z. Wang, Z. Zhang, Z. Ding, *J. Rare Earths* **28**, 241 (2010).

[7] G. Blasse, B.C. Grabmair, *Luminescent Materials*, Springer-Verlag, Berlin 1984.

[8] T. Ye, Z. Guiwen, Z. Weiping, P. Shangda, *Mater. Res. Bull.* **32**, 501 (1997).

[9] R. Schmechel, M. Kenedy, H. Vonseggem, H. Winkler, M. Kolbe, R.A. Fischer, Li Xaomao, A. Benker, M. Winter, *J. Appl. Phys.* **89**, 1679 (2001).

[10] Q. Li, L. Gao, D. Yan, *Chem. Mater.* **11**, 533 (1999).

[11] H. Tomaszewski, H. Weglarz, R.D. Gryse, *J. Eur. Ceram. Soc.* **17**, 403 (1997).

[12] T. Ye, Z. Guiwen, Z. Weiping, X. Shangda, *Mater. Res. Bull.* **32**, 501 (1997).

[13] R. Srivinivasan, R. Yogamalar, A. Chandra Bose, *Mater. Res. Bull.* **45**, 1165 (2010).

[14] L.L. Hench, J.K. West, *Chem. Rev.* **90**, 33 (1990).

[15] C. Cannas, M. Casu, A. Lai, A. Musinu, G. Piccaluga, *Phys. Chem. Chem. Phys.* **4**, 2286 (2002).

[16] L. Kepinski, M. Wolcyrz, M. Drozd, *Mater. Chem. Phys.* **96**, 353 (2006).

[17] P. Aghamkar, S. Duhan, M. Singh, N. Kishore, P.K. Sen, *J. Sol–Gel Sci. Technol.* **46**, 17 (2008).

[18] R.G. Haire, L. Eyring, *Comparisons of the Binary Oxides, Handbook on the Physics and Chemistry of Rare Earths*, North-Holland, Amsterdam 1994.

[19] H. Wang, M. Yu, C.K. Lin, J. Lin, *J. Colloid Interf. Sci.* **300**, 176 (2006).

[20] D.-M. Smilgies, *J. Appl. Crystallogr.* **42**, 1030 (2009).

[21] R. Ramamoorthy, S. Ramasamy, D. Sundaraman, *J. Mater. Res.* **14**, 90 (1999).

[22] S. Xiaoyi, Z. Yuchun, *Rare Met.* **30**, 33 (2011).